Original Research

Homotopy of resting-state functional connectivity correlates with psychological distress in adolescent and young adult cancer patients

Jianfei Xie[1], Lijun Li[2,*,†], Lu Wang[2], Panpan Xiao[2], Jin Liu[3], Xiangyu Liu[4], Jianda Zhou[1], Yunjie Liao[5,*,†], Andy SK Cheng[6]

[1]*Department of Nursing, The Third Xiangya Hospital, Central South University, 410000 Changsha, Hunan, China,* [2]*Xiangya Nursing School, Central South University, 410000 Changsha, Hunan, China,* [3]*School of Computer Science and Engineering, Central South University, 410000 Changsha, Hunan, China,* [4]*Department of Health Management Center, Hunan Cancer Hospital, 410000 Changsha, Hunan, China,* [5]*Department of Radiology, The Third Xiangya Hospital, Central South University, 410000 Changsha, Hunan, China,* [6]*Department of Rehabilitation Sciences, The Hong Kong Polytechnic University, 999077 Kowloon, Hong Kong*

TABLE OF CONTENTS

1. Abstract

Background: Adolescent and young adult cancer patients (AYACPs) experience a high incidence of psychological distress. However, the effect of psychological distress on the functional connectivity between the hemispheres in AYACPs remains unknown. Voxel-mirrored homotopy connectivity detection is an effective way to explore the effects of psychological distress on functional connectivity throughout the brain in AYACPs. **Methods**: Twenty-four AYACPs underwent structural magnetic resonance imaging. **Results**: Voxel-mirrored homotopy connectivity in the psychological distress group was significantly lower in the superior parietal gyrus, middle frontal gyrus (orbital part), superior frontal gyrus (dorsolateral), superior occipital gyrus, precuneus, lingual gyrus, calcarine fissure and surrounding cortex than in the non-psychological distress group, while in the inferior temporal gyrus and middle frontal gyrus (orbital part), voxel-mirrored homotopy connectivity was significantly higher ($p < 0.05$). ROC curve analysis showed that the decrease in voxel-mirrored homotopy connectivity in the following brain regions was helpful in distinguishing the psychological distress group from the non-psychological distress group: left superior frontal gyrus (dorsolateral), left calcarine fissure and surrounding cortex, right postcentral gyrus, and left precuneus. **Conclusions**: Activity imbalances in multiple brain regions exist in AYACPs with psychological distress. Voxel-mirrored homotopy connectivity detection is an effective way to explore the potential neural mechanisms of mental disorders in AYACPs and optimize the treatment of mental disorders.

Submitted: 15 August 2021 Revised: 1 November 2021 Accepted: 2 November 2021 Published: 30 December 2021

2. Introduction

Patients diagnosed with cancer between 15–39 years old are defined as adolescent and young adult cancer patients (AYACPs) [1]. More than 1 million new diagnoses of cancer in adolescents and young adults occur annually worldwide [2]. The overall 5-year survival rate for AYACPs has exceeded 80% with the development of cancer screening and medical technology [3]. AYACPs have more opportunities to confront physical, medical and financial challenges during the diagnosis and treatment of cancer [4, 5]. Adolescence and young adulthood are important transitional phases of life with many essential developmental changes. During this time, being diagnosed with cancer may cause unique developmental challenges at this particularly vulnerable point for them [6]. The prevalence and severity of psychological distress (PD) are higher and more common among AYACPs [7, 8]. They suffer from all kinds of psychological problems, including psychological distress, anxiety and depression [5, 9]. Neuroimaging studies have also suggested that poorer psychosocial outcomes are manifestations of brain network disruptions [10, 11]. Although clinical scales are available to measure mental status, AYACPs may not report these due to cancer shame [12]; moreover, the scales are subjective and cannot objectively reflect the psychological state of patients. Psychological distress affects the progression, prognosis and treatment outcome of cancer [13]. Objective and accurate early identification of psychological distress in AYACPs is beneficial to cancer treatment. Functional changes in brain regions and neural circuits in patients with psychological distress can be provided by neuroimaging studies that provide insight and explore the neuropathology of physiological disorders in AYACPs.

Resting-state functional magnetic resonance imaging (fMRI) has shown abnormal activity or functional connectivity in many brain regions, including the frontal lobe (dorsolateral prefrontal cortex, DLPFC; ventrolateral prefrontal cortex, VLPFC; ventromedial prefrontal cortex, VMPFC), limbic system (anterior cingulate cortex, ACC; amygdala; hippocampus), thalamic striatum (thalamus; globus pallidus; nucleus accumbens; putamen; caudate nucleus) and insula among youth or elderly healthy or depressive subjects [14–17]. Raichle *et al*. [18] analyzed the oxygen extraction fraction (OEF), cortical blood flow (CBF) and BOLD signals from positron emission imaging (PET) and fMRI data in normal adult human. Based on the signal characteristics in the active state of the resting-state fMRI, the concept of a default mode network (DMN) was obtained. This network mainly includes the posterior cingulate cortex/precuneus (PCC/PCUN), medial prefrontal cortex (MPFC), bilateral angular cortex and lateral temporal gyrus, temporal cortex, and hippocampus [19]. These structures or systems are mainly involved in emotional processing, cognitive control, self-instruction, emotional cognition and reward processing, especially in the process of nonadaptive rumination in the face of negative emotional stimulation [20].

Patients with PD present abnormal network activity, functional connectivity or network attributes in multiple cortices or subcortical areas, such as amplitude of low-frequency fluctuations (ALFF) in the cerebellum and striatum and disruptions in local homogeneity (ReHo), voxel-mirrored homotopy connectivity (VMHC), functional connectivity and small-world network attributes in the prefrontal lobe, orbitofrontal gyrus, anterior cuneiform lobe, insula, and limbic system brain areas (such as the ACC, amygdala and hippocampus) [21, 22]. VMHC is a kind of resting state functional magnetic resonance imaging (rs-fMRI) method developed in recent years that analyzes the synchronous activity between the two hemispheres. Homotopy refers to the highly similar endogenous spontaneous activities of neurons of the same origin in the left and right hemispheres. This is one of the important features of the internal functional framework of the brain. Reflections in the mode of information communication between the two hemispheres of the brain is very important for the brain information integration function. Homotopy is also a potential mechanism of human cognitive and behavioral coherence [23]. It has been gradually applied to the research of many central nervous system diseases and mental disorders [23, 24].

Compared with the healthy population, patients with PD have decreased brain activity in the limbic system and increased activity in the frontal-temporal cortex [25–27]. Abnormal activity in these brain regions is involved in top-down (high-level emotional cognitive processing) and bottom-up (coding perceptual information resulting in emotional stimulation) regulatory abnormalities in the prefrontal subcortical loop [28]. These abnormal brain activities are presented in multiple mental disorders, such as depression [29], bipolar disorder [27], anxiety, posttraumatic stress disorder [30] and borderline personality disorder [31]. These disruptions may be different across the above-mentioned diseases in various forms and degrees of emotional regulation abnormalities. However, the differences involve the cognitive control network, the participation of the reward loop and the emotional volatility (such as bipolar disorder) [32].

The theoretical framework of this study is research domain criterion (RDoC), a brain-centered research strategy, developed by National Institute of Mental Health (NIH) (2021). RDoC is a study framework for understanding mental disorders. It incorporates various levels of knowledge (from genomics and circuitry to behavior and self-report) to investigate the fundamental functional dimensions that span the full range of human behavior from normal to abnormal. The aim of this research strategy is to establish a classification system for mental disorders based on brain mechanisms. According to the idea of RDoC, a brain-centered, neuroimaging-based mind-brain associ-

ation research framework was developed. This research framework emphasizes the use of brain functional networks as the starting point for establishing research hypotheses and inferring the psychological and behavioral characteristics associated with a particular brain functional network.

Fan *et al*. [33] experienced that linking the course of depression to changes in brain function can help understand the neural structure of major depression in adults. Another previous study also showed that the correlation between cognitive performance and homotopy in health adults [34]. However, the effect of PD on the functional connectivity between the hemispheres in AYACPs remains unknown. This study attempted to explore changes in homotopy of resting-state functional connectivity between hemispheres among AYACPs with PD by identifying focal lesions in VMHC and distinguishing patients with and without PD based on these regions.

3. Materials and methods

3.1 Setting and participants

This study is a cross-sectional design. Participants were enrolled and data were collected between March 2018 and August 2019 in the hospital. Twenty-four AYACPs were included. The inclusion criteria required that participants (1) were aged 15–39 years; (2) had a primary diagnosis of cancer (cervical, ovarian, uterine, lung or nasopharyngeal carcinoma) within the previous 3 months; (3) knew their disease diagnosis; (4) had strong right-handedness according to the Edinburgh Hands Survey [35]; and (5) were native Chinese speakers. Participants were excluded if they (1) had reported a history of central nervous system injuries, such as brain damage or congenital dementia; (2) had physical diseases that could have damaged cognitive function, such as cerebral hemorrhage, chronic pain, severe vision or hearing impairment, or limb disorders; and (3) had any contraindications for fMRI scanning, such as strong magnetic objects in the body or claustrophobia.

Eligible participants were screened by the Distress Thermometer (DT) before 8:00 AM, which was before the daily rounds (approximately 8:30 AM) to minimize the effects of treatment or the patients' routine on their psychological condition. The DT is recommended by the National Comprehensive Cancer Network for cancer patients. Cancer patients' psychological distress was measured by an 11-point numerical simulation thermometer (0 = no distress, 10 = extreme distress) [36]. According to current guidelines, a score of 4 or more is considered to be associated with clinical psychological distress [37]. The participants were divided into two groups: the PD group with a DT score $\geq$4 vs. the NPD group. Each participant completed a psychological assessment and rs-fMRI scan on the same day after screening, separated by at least half an hour. The ethics committees approved this study. All participants volunteered to participate in the study and provided written informed consent.

3.2 Measures

3.2.1 Hospital anxiety and depression scale (HADS)

The HADS was developed by Zigmond & Snaith [38]. Screening patient anxiety and depression, widely used in cancer patients in hospitals with mental disorders [39, 40]. The HADS comprised 14 items in total using a 4-point Likert scoring system (not at all = 0, almost all the time = 3). Of these items, 7 items were used to assess anxiety (HADS-A), and 7 items were used to assess depression (HADS-D). A higher score indicated more severe anxiety or depression. The total score of the subscale can range from 0 to 21: 0–7 = negative; 8–10 = light; 11–14 = moderate; 15–21 = severe. The Cronbach's α of the Chinese version of the HADS scale is 0.919, and the Cronbach's α of the subscales are both approximately 0.85 [41].

3.2.2 MRI data acquisition

The International Cognition and Cancer Task Force (ICCTF) has proposed that a high-resolution T1-weighted anatomical MRI scan and rs-fMRI should be contained in a minimal set of MRI sequences to evaluate functional brain networks [42]. In the hospital, the brain rs-fMRI data were gathered on a Philips 3 T scanner (Ingenia, Philips Healthcare, Best, NL) applying a head coil of 8-channel SENSE. The participants were instructed to close their eyes and relax throughout rs-fMRI data acquisition. A gradient echo-planar imaging (EPI) sequence was used to obtain blood-oxygen-level-dependent (BOLD) fMRI data. The EPI sequence parameters were as follows: repetition time/echo time (TR/TE) = 2000/30 msec, thickness = 4 mm, field of view (FOV) = 224 $\times$ 224 mm, flip angle = 90°, matrix = 64 $\times$ 62, slices = 36, gap = 0, slice order = interleaved, volumes = 200 and time = 410 s. T1-weighted imaging was achieved for morphometric (GM volume, cortical thickness and surface area) analyses using a three-dimensional high resolution T1WI sequence. This T1WI sequence parameters were as follows: repetition time (TR)/echo time (TE) = 7.8/2.3 ms; slices = 226; thickness = 1 mm; gap = 0 mm; flip angle (FA) = 7°; acquisition matrix = 240 $\times$ 240; the structural sequence took 376 s.

3.2.3 The preprocessing of MRI data

Rs-fMRI images are preprocessed through the graph theory network analysis toolbox of image connectives (GRETNA) [43]. In this study, imaging data processing was mainly based on the MATLAB platform (MATLAB R2015b, The MathWorks, Inc., Natick, Mass). Data Processing Assistant for Resting-state fMRI (DPARSF 2.3) was used to preprocess the functional images [44, 45]. The graphical user interface (GUI) of Statistical Parameter Mapping (SPM12) was used to integrate and visualize the necessary steps of fMRI data.

Before preprocessing, each volume's first ten time points of fMRI data were removed to avoid instability in the initial magnetic field. The remaining rs-fMRI images were processed in sequence as follows: (1) the 35th plane was used as the reference plane to carry out slice timing to control the time difference across different scanning plane images at the same time point, and a spatial correction to control the head motion effect of different time points of image acquisition was carried out. Participants with head motion exceeding a maximum displacement of 1.5 mm or 1.5-degree angular motion in any direction were excluded from the study. (2) T1 images were registered to functional images and then reoriented. (3) For spatial normalization, T1-weighted anatomical images were divided into white matter, gray matter and cerebrospinal fluid and then passed through 12 parametric nonlinear affine transformations that standardized the images of each subject into the Montreal Neurological Institute (MNI) space. The above transformation parameters were applied to the functional images, and then the functional images were resampled to $3 \times 3 \times 3$ mm^3 isotropic voxels. (4) Space was smoothed with 6-mm full-width at half-maximum (FWHM) isotropic Gaussian kernels. (5) The linear trend of each voxel in the whole time series was removed. (6) The nontarget signal (white matter signal, CSF signal number, 6 head motion parameters) was transformed, and peak regressions were removed from the original time series. (7) A low-frequency bandpass filter (0.01–0.08 Hz) was used to denoise, by eliminating artifacts, minimizing low-frequency drift, and removing high-frequency noise (physiological noise such as breathing and heartbeat).

To calculate the VMHC between symmetrical voxels across hemispheres of the brain, the preprocessed functional image was converted into symmetrical space using the following procedures: (1) averaging standardized gray matter images of all subjects to generate the average image; (2) averaging the above-average image with bilateral mirror templates to create a group-specific symmetrical template; and (3) registering each standardized gray matter image to the generated symmetrical template and then transforming the functional image based on a nonlinearity strategy. VMHC at the individual level was calculated from the symmetrical unilateral gray matter hemispheric template. Pearson correlation analysis was conducted between each voxel and its corresponding voxel in the mirror-symmetric hemispheres of each subject. Then, the Fisher *z* transform was applied to the calculated correlation coefficients to obtain the standardized distribution data. Finally, the VMHC values used for statistical analysis were generated. The above steps were carried out in DPARSF 2.3 software. VMHC was calculated based on bilateral symmetrical brain regions, so the coordinates of peak points of corresponding brain regions on the left and right also correspond to each other.

3.3 Statistical analysis

All statistical analyses were performed by SPSS software for Windows (version 24.0, IBM Corp., Armonk, NY, USA). Descriptive statistics, ANOVAs, independent samples *t*-tests, Kruskal-Wallis tests, and χ^2 tests were used to determine whether participants' characteristics (sociodemographic and clinical) were different across experimental conditions and HADS scores.

The regional differences in VMHC were determined by analysis of covariance. In the unilateral hemisphere of the symmetrical template, AlphaSim analysis determined by Monte Carlo simulation was used to correct the VMHC results for multiple comparisons. The AlphaSim program is part of a standard neuroimaging toolbox of the Analysis of Functional NeuroImages (AFNI) (Linux, Ubuntu 18.04, NIH, USA) (http://afni.nimh.nih.gov) and is one of the methods for multiple comparison correction combining voxel intensity and cluster extent. In AlphaSim, Monte Carlo permutation simulations were applied to estimate the null distribution [46]. Specifically, the algorithm generates an estimate of the overall significance level achieved for various combinations of probability thresholds and cluster size thresholds by iteration of the process of random image generation, Gaussian filtering, thresholding, image masking, and tabulation of cluster size frequencies. However, the algorithm of AlphaSim is different from the abovementioned [47]. We thought that it does provide the appropriate cluster-level threshold to achieve the desired false-positive rate. Moreover, AlphaSim has been widely used in the published literature about psychological distress [48, 49]. The threshold was set as $p < 0.005$, the voxel level $p < 0.01$ was used in the correction, and the cluster size was $\geq$26 voxels (AFNI, http://afni.nimh.nih.gov/pub/dist/doc/manual/AlphaSim.pdf) [44, 45].

After obtaining the time series in the brain areas that were different, the relationship between VMHC and patient psychological characteristics was examined by bivariate Pearson's or Spearman correlation analysis. Area under the curve (AUC) analysis of receiver operating characteristic (ROC) curves was used to determine the best thresholds to distinguish PD from NPD and was characterized as follows: 0.9–1.0 = excellent; 0.8–0.9 = very good, 0.7–0.8 = good; 0.6–0.7 = weak; And 0.5–0.6 = poor [50]. For the ROC analysis of multi-index combinations, the binary logistic regression method was used to calculate the prediction value of the joint index. Values of $p < 0.05$ was applied to determine statistically significant differences in this study.

4. Results

Fifteen participants with PD and nine participants with NPD were recruited. There was no significant difference between the two groups in the demographic characters. Table 1 summarizes their demographics and clinical characteristics.

Table 1. Group differences in demographics and clinical characteristics (N = 24).

Variables	N (Percentages, %)/Mean ± SD		Z	*p*
	PD (N = 15)	NPD (N = 9)		
Gender (M/F)	5/10	3/6	–0.533	0.594
Age (years)	31.87 ± 2.90	29.33 ± 5.32	–1.351	0.177
Education			–0.573	0.567
Junior high school or below	6 (40)	3 (33)		
High school	5 (33)	4 (44)		
Diploma	4 (27)	2 (23)		
Cancer type			–0.310	0.757
Cervical cancer	9 (60)	5 (56)		
Ovarian cancer	2 (13)	1 (11)		
Tongue cancer	1 (7)	/		
Lung cancer	2 (13)	2 (22)		
Nasopharyngeal cancer	1 (7)	1 (11)		
Cancer stage			–0.156	0.876
Stage I–IIa	13 (87)	8 (89)		
Stage IIb–IIIa	2 (13)	1 (11)		
Treatment type			–0.876	0.381
Surgery	9 (60)	7 (78)		
Surgery + Chemotherapy	6 (40)	2 (22)		

Note: NPD, Non-Psychological distress; PD, Psychological distress.

4.1 VMHC difference between PD and NPD groups

The results showed 16 regional changes between PD and NPD. Compared with the PD group, the NPD group had considerably declined VMHC values in the middle frontal gyrus (orbital part) and bilateral inferior temporal gyrus, but significantly increased values in the superior parietal gyrus, middle frontal gyrus (orbital part), superior frontal gyrus (dorsolateral) (SFGdor), superior occipital gyrus, precuneus, lingual gyrus, calcarine fissure and surrounding cortex (Table 2 and Fig. 1). As shown in Table 3, PD and NPD groups were significantly different in anxiety and depression ($p < 0.05$). Negative correlations were found between decreased VMHC in some brain areas and HADS-D scores: bilateral superior parietal gyrus (left: $r = –0.576$, $p = 0.025$; right: $r = –0.522$, $p = 0.046$) and left superior frontal gyrus (dorsolateral) ($r = –0.563$, $p = 0.029$) (Table 4). There were no significant correlations between VMHC values in abnormal brain regions and HADS total scores or HADS-A scores ($p > 0.05$).

4.2 Efficacy of brain area differences in VMHC in distinguishing PD and NPD

ROC curve analysis demonstrated that four regions of VMHC changes could identify patients with PD. They were the left SFGdor (AUC = 0.681, $p = 0.014$, sensitivity = 0.444, specificity = 0.40; see Fig. 2A), left calcarine fissure and surrounding cortex (AUC = 0.614, $p = 0.036$, sensitivity = 0.867, specificity = 0.222; see Fig. 2B), right postcentral gyrus (PoCG) (AUC = 0.651, $p = 0.022$, sensitivity = 0.800, specificity = 0.444; see Fig. 2C) and left precuneus (AUC = 0.629, $p = 0.029$, sensitivity = 0.800, specificity = 0.333; see Fig. 2D). The combined ROC anal-

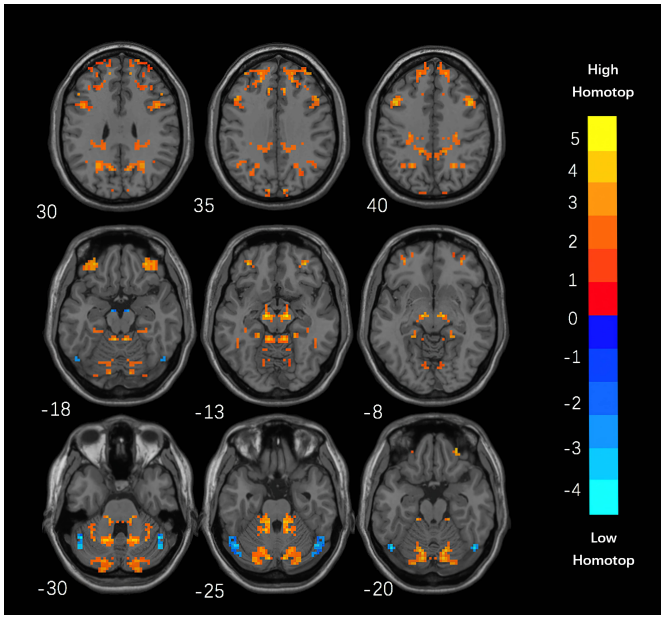

Fig. 1. Brain area with VMHC difference between PD and NPD. * *Note:* The VMHC of PD was lower in superior parietal gyrus, middle frontal gyrus, superior frontal gyrus, dorsolateral, superior occipital gyrus, precuneus, lingual gyrus, calcarine fissure and surrounding cortex than that of NPD, while the VMHC value of PD in inferior temporal gyrus and middle frontal gyrus (orbital part) was higher. The figure in the lower left corner represents the *z* coordinate value of the coordinate system of Montreal Institute of Neurology, and the icon on the right represents the T value ($p < 0.05$, AlphaSim correction $p < 0.01$, cluster volume ≥32 voxel). ***Abbreviations*: NPD, Non-Psychological distress; PD, Psychological distress; VMHC, voxel-mirrored homotopy connectivity.

Table 2. Brain regions with VMHC differences between PD and NPD (N = 24).

Region	Number of voxels	Peak MNI coordinate			T
		X	Y	Z	
PD > NPD					
ITG.R	9	45	–66	–27	–4.4788
ITG.L	7	–45	–66	–27	–4.4788
ORBsupmed.R	46	27	45	–21	–4.3893
ORBsupmed.L	24	–33	45	–12	–3.8578
PD < NPD					
CAL.R	54	24	–21	9	5.572
CAL.L	36	–24	–21	9	5.572
LING.R	28	6	–78	–3	5.1997
LING.L	27	–6	–78	–3	5.1997
MFG.R	127	42	12	42	4.1998
FGdor.L	222	–42	12	42	4.1998
SOG.R	24	15	–99	21	4.4679
SOG.L	27	–15	–99	21	4.4679
PCUN.R	67	15	–57	51	4.2652
PCUN.L	69	–15	–57	51	4.2652
SPG.L	22	–18	–72	60	3.1435
SPG.R	32	18	–72	63	3.2036

Note: 1 voxel = 3 × 3 × 3 mm^3; CAL, Calcarine fissure and surrounding cortex; ITG, Inferior temporal gyrus; L, Left; LING, Lingual gyrus; MFG.R, Middle frontal gyrus; MNI, the Montreal Neurological Institute; ORBsupmed, Middle frontal gyrus, orbital part; PCUN, Precuneus; R, Right; SFGdor, Superior frontal gyrus, dorsolateral; SOG, Superior occipital gyrus; SPG, Superior parietal gyrus; T, peak point T value; VMHC, Voxel-mirrored homotopic connectivity.

Table 3. The psychological characteristic of PD and NPD (N = 24).

Region	PD	NPD	*t*	*p**
HADS	16.867 ± 3.021	8.333 ± 4.062	5.890	<0.001
HADS-A	8.933 ± 2.502	4.444 ± 2.404	4.870	<0.001
HADS-D	7.933 ± 1.981	3.889 ± 2.083	4.747	<0.001

Note: HADS, Hospital anxiety and depression scale; HADS-A, Hospital anxiety and depression scale-Anxiety; HADS-D, Hospital anxiety and depression scale-Depression; NPD, Non- Psychological distress; PD, Psychological distress. * $p < 0.001$.

Table 4. Correlation of HADS-D and abnormal VMHC brain regions of PD (N = 15).

Region	HADS-D	
	r	*p**
SFGdor.L	–0.563	0.029
SPG.L	–0.576	0.025
SPG.R	–0.522	0.046

Note: HADS-D, Hospital anxiety and depression scale-Depression; L, Left; R, Right; SFGdor, Superior frontal gyrus, dorsolateral; SPG, Superior parietal gyrus. * $p < 0.05$.

ysis showed that the combined index had a better discrimination effect and more balanced sensitivity and specificity in predicting PD patients when the VMHC characteristics of these four regions were integrated and collected (AUC = 0.704, $p = 0.027$, sensitivity = 0.733, specificity = 0.667; Fig. 2E).

5. Discussion

The current study found that an increased in the middle frontal gyrus (orbital part) and inferior temporal gyrus of VMHC values among AYACPs with PD compared to those without PD in VMHC. The middle frontal gyrus (orbital part) is a part brain area of the frontal limbic loop, which is mainly involved in the processing of conditioned emotion [51] and the rumination process [52]. These loops ensure the formation of normal emotions by coordinating emotions and external stimulation [53]. The increase in VMHC in the orbital part of the middle frontal gyrus (orbital part) may promote the generation of depressive symptoms by mediating the rumination process associated with poor emotional regulation and nonadaptive thinking [26]. In addition, graph theory research has also found that the right middle frontal gyrus (orbital part), which significantly presented lower homotopy in our study, relative to the emotion-related region [54]. Abnormal VMHC in these areas may be a compensatory effect for the readjustment to emotional dysfunction.

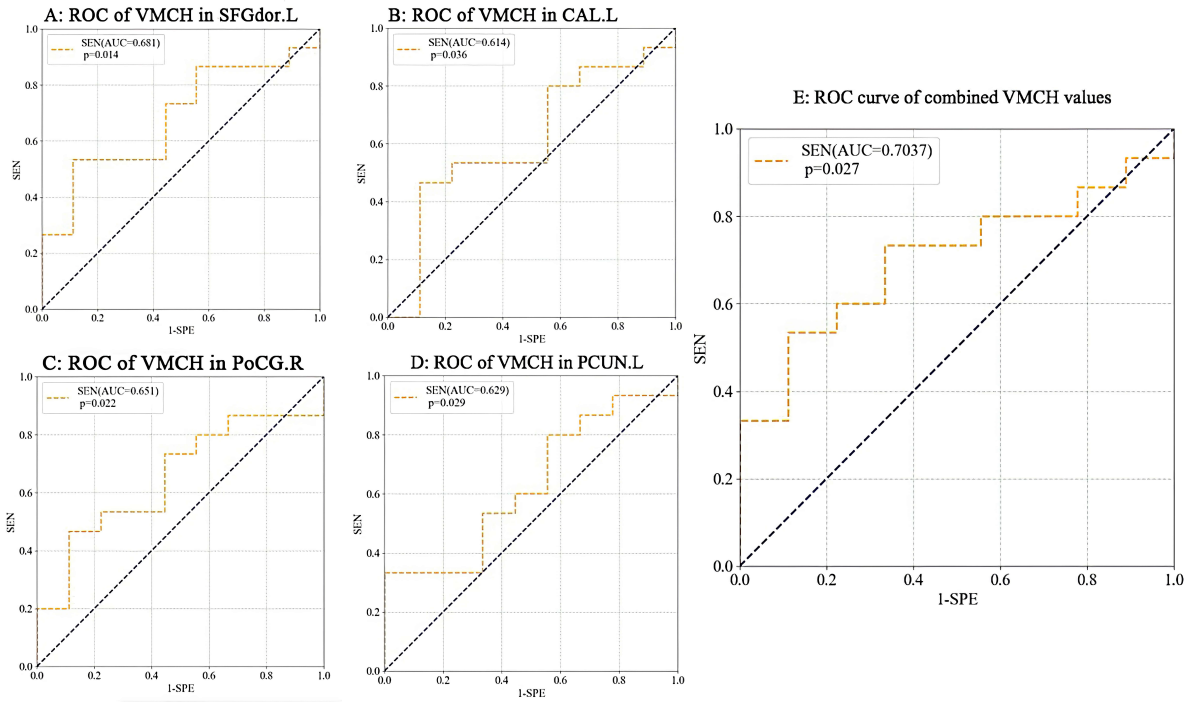

Fig. 2. ROC analysis of VMHC in the altered regions as a potential means to differentiate between PD and NPD. (A) The ROC curve of VMCH in SFGdor.L, AUC = 0.681, p = 0.014, sensitivity = 0.444, specificity = 0.40; (B) The ROC curve of VMCH in CAL.L, AUC = 0.614, p = 0.036, sensitivity = 0.867, specificity= 0.222; (C) The ROC curve of VMCH in PoCG.R, AUC = 0.651, p = 0.022, sensitivity = 0.800, specificity = 0.444; (D) The ROC curve of VMCH inPCUN.L, AUC = 0.629, p = 0.029, sensitivity = 0.800, specificity = 0.333; (E) The ROC curve of combined VMCH values, AUC = 0.704, p = 0.027, sensitivity = 0.733, specificity = 0.667, which had a better discrimination effect and more balanced sensitivity and specificity in predicting PD patients.

We discovered 16 regions of functional connectivity between the two hemispheres that changed among AYACPs with PD. Compared with cancer patients in other age groups, AYACPs with PD presented different focally disrupted sites [17, 55]. Compared to healthy controls, depressed adolescents showed reduced resting-state functional connectivity in the dorsolateral prefrontal cortex (DLPFC) and the ventromedial prefrontal cortex (VMPFC) [56]. Similarly, VMHC in the PD group was significantly lower in the superior frontal gyrus than in the NPD group in this study, suggesting that adolescent depression may be characterized by dysfunction of frontolimbic circuits underpinning emotional regulation. Moreover, the abnormal range of information exchange between hemispheres in the AYACPs with PD was larger than that in normal people with PD of the same age [57]. The unique pattern of VMHC changes between the PD and NPD groups suggests that abnormal information exchange between hemispheres may be the neural basis of psychological distress in AYACPs. These changes provide a new perspective to recognize and understand the heterogeneity of neurological changes among different populations.

We also found that the decrease in VMHC in the left DLPFC and bilateral superior parietal gyrus was significantly negatively correlated with the severity of depression in the PD group. When emotional impulses are produced in the marginal center, emotional expression is restricted by the prefrontal cortex. The two sides of the prefrontal cortex seem to be responsible for controlling different emotional responses. The right side regulates depression-related emotions, and the left side regulates relatively positive emotions. Normann *et al*. [58] hypothesized that one aspect of the pathogenesis of depressive disorder is hypofunction of the left brain and hyperactivity of the right brain. Effectively stimulating the excitability of the left superior frontal gyrus (dorsolateral) can relieve patients' depression [59].

The results revealed the possibility of distinguishing NPD and PD based on some of the differences in VMHC. ROC analyses showed that the changes in VMHC in the SFGdor, CAL, PoCG and PCUN can objectively and effectively identify cancer patients with PD. When the VMHC changes in the four regions were integrated, a more optimized discrimination ability was revealed. This demonstrated that the synergism of multiple brain regions may be involved in the compensation of neurological changes caused by PD, and the change in functional coordination between hemispheres may not only be related to early response to psychological distress but also may affect PD by mobilizing the reserve in brain function activity in these regions. Additionally, as questionnaires have been criticized for their subjectivity, being easily affected by the environment and limited by participants' conditions, this re-

sult identified an objective psychological testing method that can be applied in further understanding AYACPs' psychological distress.

The strengths of this study include applying objective indicators to the study of psychological distress in AYACPs. However, the current study has a few limitations that need to be addressed. First, we did not establish a group of healthy controls, that is, there was an absence of normal people without PD. We cannot identify whether the severity of the emotional disorder is related to the functional imbalance in particular brain regions. Second, this study was conducted with AYA patients receiving treatments, and VMHC changes cannot eliminate the disease effects. Moreover, the small sample size may have decreased the authority to notice functional differences. We targeted on AYACPs, which was scarcely investigated the correlation between their psychological distress and functional connectivity before. Our study could serve as a preliminary investigation of this important but overlooked correlation among AYACPs.

6. Conclusions

The characteristic differences in the mirrored homotopic connectivity between the PD group and NPD group will support us in understanding the neural mechanisms of PD. VMHC detection is an effective method to explore the potential neural mechanisms of mental disorders in AYACPs and optimize the treatment of mental disorders. Meanwhile, VMHC abnormalities in the SFGdor, calcarine fissure and surrounding cortex, PoCG and PCUN regions are correlate with psychological distress for AYACPs, which may contribute to promoting the realization of objective psychological testing.

7. Author contributions

JX the primary author, led the work conception and design of the study. LL and YL the corresponding authors, analysis, interpretation of data and drafting the article. LW, PX, JL and JZ organized the survey, revised the paper and provided constructive suggestion. LL, YL and XL analyzed data and revised it critically for important content. ASKC revised the paper critically for important intellectual content.

8. Ethics approval and consent to participate

All procedures performed in the trial were in accordance with the ethical standards of the Third Xiangya Hospital, Central South University IRB. This study was approved by the ethics committee of The Third Xiangya Hospital of Central South University (No. 2018-S039). All participants have signed the informed consent form.

9. Acknowledgment

We would like thanks to Wisdom Accumulation and Talent Cultivation Project, National Natural Science Foundation of China and Fundamental Research Funds for the Central Universities of Central South University fund project for their finical supports. And grateful to all participants for their voluntary participation and all the members of our research team.

10. Funding

Paper supported by the Wisdom Accumulation and Talent Cultivation Project of the Third Xiangya Hospital of Central South University (NO. YX202006); The National Natural Science Foundation of China (NO. 82073409); Fundamental Research Funds for the Central Universities of Central South University (No. 2020zzts841).

11. Conflict of interest

The authors declare no conflict of interest.

12. References

[1] Mitchell L, Stuart-McEwan T, Panet H, Gupta A. Adolescents and Young Adults: Addressing Needs and Optimizing Care with a Clinical Nurse Specialist. Clinical Journal of Oncology Nursing. 2017; 21: 123–126.

[2] World Health Organization. Estimated number of new cases in 2020, worldwide, both sexes, ages 15–39. 2020. Available at: https://gco.iarc.fr/today/online-analysis-table?v=2020&mode=cancer&mode_population=continents&population=900&populations=900&key=asr&sex=0&cancer=39&type=0&statistic=5&prevalence=0&population_group=0&ages_group%5B%5D=3&ages_group%5B%5D=7&group_cancer=1&include_nmsc=1&include_nmsc_other=1 (Accessed: 6 June 2021).

[3] Keegan THM, Ries LAG, Barr RD, Geiger AM, Dahlke DV, Pollock BH, *et al*. Comparison of cancer survival trends in the United States of adolescents and young adults with those in children and older adults. Cancer. 2016; 122: 1009–1016.

[4] Mishra SI, Rishel Brakey H, Kano M, Nedjat-Haiem FR, Sussman AL. Health related quality of life during cancer treatment: Perspectives of young adult (23–39 years) cancer survivors and primary informal caregivers. European Journal of Oncology Nursing. 2018; 32: 48–54.

[5] Jim HSL, Jennewein SL, Quinn GP, Reed DR, Small BJ. Cognition in Adolescent and Young Adults Diagnosed with Cancer: an Understudied Problem. Journal of Clinical Oncology. 2018; 36: 2752–2754.

[6] Kaul S, Avila JC, Mutambudzi M, Russell H, Kirchhoff AC, Schwartz CL. Mental distress and health care use among survivors of adolescent and young adult cancer: a cross-sectional analysis of the National Health Interview Survey. Cancer. 2017; 123: 869–878.

[7] Xie J, Ding S, He S, Duan Y, Yi K, Zhou J. A Prevalence Study of Psychosocial Distress in Adolescents and Young Adults with Cancer. Cancer Nursing. 2017; 40: 217–223.

[8] Geue K, Brähler E, Faller H, Härter M, Schulz H, Weis J, *et al*. Prevalence of mental disorders and psychosocial distress in Ger-

man adolescent and young adult cancer patients (AYA). Psycho-Oncology. 2019; 27: 1802–1809.
[9] Geue K, Göbel P, Leuteritz K, Nowe E, Sender A, Stöbel-Richter Y, *et al*. Anxiety and depression in young adult German cancer patients: Time course and associated factors. Psycho-Oncology. 2019; 28: 2083–2090.
[10] Ho TC, Yang G, Wu J, Cassey P, Brown SD, Hoang N, *et al*. Functional connectivity of negative emotional processing in adolescent depression. Journal of Affective Disorders. 2014; 155: 65–74.
[11] Mayberg HS. Defining the neural circuitry of depression: toward a new nosology with therapeutic implications. Biological Psychiatry. 2007; 61: 729–730.
[12] Kim MA, Yi J. Life after cancer: how does public stigma increase psychological distress of childhood cancer survivors? International Journal of Nursing Studies. 2015; 51: 1605–1614.
[13] Herschbach P, Keller M, Knight L, Brandl T, Huber B, Henrich G, *et al*. Psychological problems of cancer patients: a cancer distress screening with a cancer-specific questionnaire. British Journal of Cancer. 2004; 91: 504–511.
[14] Hamilton JP, Etkin A, Furman DJ, Lemus MG, Johnson RF, Gotlib IH. Functional neuroimaging of major depressive disorder: a meta-analysis and new integration of base line activation and neural response data. The American Journal of Psychiatry. 2013; 169: 693–703.
[15] Miller CH, Hamilton JP, Sacchet MD, Gotlib IH. Meta-analysis of Functional Neuroimaging of Major Depressive Disorder in Youth. JAMA Psychiatry. 2016; 72: 1045–1053.
[16] Müller VI, Cieslik EC, Serbanescu I, Laird AR, Fox PT, Eickhoff SB. Altered Brain Activity in Unipolar Depression Revisited: Meta-analyses of Neuroimaging Studies. JAMA Psychiatry. 2017; 74: 47–55.
[17] Weber K, Giannakopoulos P, Delaloye C, de Bilbao F, Moy G, Ebbing K, *et al*. Personality traits, cognition and volumetric MRI changes in elderly patients with early-onset depression: a 2-year follow-up study. Psychiatry Research. 2013; 198: 47–52.
[18] Raichle ME, MacLeod AM, Snyder AZ, Powers WJ, Gusnard DA, Shulman GL. A default mode of brain function. Proceedings of the National Academy of Sciences of the United States of America. 2001; 98: 676–682.
[19] Fox MD, Snyder AZ, Vincent JL, Corbetta M, Van Essen DC, Raichle ME. The human brain is intrinsically organized into dynamic, anticorrelated functional networks. Proceedings of the National Academy of Sciences of the United States of America. 2005; 102: 9673–9678.
[20] Hamilton JP, Farmer M, Fogelman P, Gotlib IH. Depressive Rumination, the Default-Mode Network, and the Dark Matter of Clinical Neuroscience. Biological Psychiatry. 2016; 78: 224–230.
[21] Lai C, Wu Y. Decreased inter-hemispheric connectivity in anterior sub-network of default mode network and cerebellum: significant findings in major depressive disorder. The International Journal of Neuropsychopharmacology. 2015; 17: 1935–1942.
[22] Zhu X, Wang X, Xiao J, Liao J, Zhong M, Wang W, *et al*. Evidence of a Dissociation Pattern in Resting-State Default Mode Network Connectivity in first-Episode, Treatment-Naive Major Depression Patients. Biological Psychiatry. 2012; 71: 611–617.
[23] Zuo X, Kelly C, Di Martino A, Mennes M, Margulies DS, Bangaru S, *et al*. Growing together and growing apart: regional and sex differences in the lifespan developmental trajectories of functional homotopy. The Journal of Neuroscience. 2010; 30: 15034–15043.
[24] Yuan K, Qin W, Liu P, Zhao L, Yu D, Zhao L, *et al*. Reduced fractional anisotropy of corpus callosum modulates inter-hemispheric resting state functional connectivity in migraine patients without aura. Public Library of Science One. 2013; 7: e45476.
[25] Siegle GJ, Steinhauer SR, Thase ME, Stenger VA, Carter CS. Can't shake that feeling: event-related fMRI assessment of sustained amygdala activity in response to emotional information in depressed individuals. Biological Psychiatry. 2002; 51: 693–707.
[26] Sheline YI, Barch DM, Donnelly JM, Ollinger JM, Snyder AZ, Mintun MA. Increased amygdala response to masked emotional faces in depressed subjects resolves with antidepressant treatment: an fMRI study. Biological Psychiatry. 2002; 50: 651–658.
[27] Phillips ML, Drevets WC, Rauch SL, Lane R. Neurobiology of emotion perception II: Implications for major psychiatric disorders. Biological Psychiatry. 2003; 54: 515–528.
[28] Ochsner KN, Ray RR, Hughes B, McRae K, Cooper JC, Weber J, *et al*. Bottom-up and top-down Processes in Emotion Generation. Psychological Science. 2009; 20: 1322–1331.
[29] Johnstone T, van Reekum CM, Urry HL, Kalin NH, Davidson RJ. Failure to regulate: counterproductive recruitment of top-down prefrontal-subcortical circuitry in major depression. The Journal of Neuroscience. 2007; 27: 8877–8884.
[30] Etkin A, Wager TD. Functional neuroimaging of anxiety: a meta-analysis of emotional processing in PTSD, social anxiety disorder, and specific phobia. The American Journal of Psychiatry. 2007; 164: 1476–1488.
[31] Hazlett EA, Zhang J, New AS, Zelmanova Y, Goldstein KE, Haznedar MM, *et al*. Potentiated amygdala response to repeated emotional pictures in borderline personality disorder. Biological Psychiatry. 2013; 72: 448–456.
[32] Malhi GS, Tanious M, Fritz K, Coulston CM, Bargh DM, Phan KL, *et al*. Differential engagement of the fronto-limbic network during emotion processing distinguishes bipolar and borderline personality disorder. Molecular Psychiatry. 2014; 18: 1247–1248.
[33] Fan H, Yang X, Zhang J, Chen Y, Li T, Ma X. Analysis of voxel-mirrored homotopic connectivity in medication-free, current major depressive disorder. Journal of Affective Disorders. 2019; 240: 171–176.
[34] Vallesi A, Visalli A, Gracia-Tabuenca Z, Tarantino V, Capizzi M, Alcauter S, *et al*. Fronto-parietal homotopy in resting-state functional connectivity predicts task-switching performance. Brain structure & function. 2021. (in press)
[35] Oldfield RC. The assessment and analysis of handedness: the Edinburgh inventory. Neuropsychologia. 1972; 9: 97–113.
[36] Comprehensive Cancer Network. NCCN Distress Thermometer and Problem List for Patients. 2021. Available at: https://www.nccn.org/docs/default-source/patient-resources/nccn_distress_thermometer.pdf?sfvrsn=ef1df1a2_4 (Accessed: 21 October 2021).
[37] Roth AJ, Kornblith AB, Batel-Copel L, Peabody E, Scher HI, Holland JC. Rapid screening for psychologic distress in men with prostate carcinoma: a pilot study. Cancer. 1998; 82: 1904–1908.
[38] Zigmond AS, Snaith RP. The hospital anxiety and depression scale. Acta Psychiatrica Scandinavica. 1983; 67: 361–370.
[39] Tan J-, Molassiotis A, Lloyd-Williams M, Yorke J. Burden, emotional distress and quality of life among informal caregivers of lung cancer patients: an exploratory study. European Journal of Cancer Care. 2018; 27: e12691.
[40] Desautels C, Savard J, Ivers H, Savard M, Caplette-Gingras A. Treatment of depressive symptoms in patients with breast cancer: a randomized controlled trial comparing cognitive therapy and bright light therapy. Health Psychology. 2018; 37: 1–13.
[41] Ferri P, Guadi M, Marcheselli L, Balduzzi S, Magnani D, Di Lorenzo R. The impact of shift work on the psychological and physical health of nurses in a general hospital: a comparison between rotating night shifts and day shifts. Risk Manag Healthc Policy. 2016; 9: 203–211.
[42] Deprez S, Kesler SR, Saykin AJ, Silverman DHS, de Ruiter MB, McDonald BC. International Cognition and Cancer Task Force Recommendations for Neuroimaging Methods in the Study of Cognitive Impairment in Non-CNS Cancer Patients. Journal of

the National Cancer Institute. 2018; 110: 223–231.
[43] Wang J, Wang X, Xia M, Liao X, Evans A, He Y. GRETNA: a graph theoretical network analysis toolbox for imaging connectomics. Frontiers in human neuroscience. 2015; 9: 386.
[44] Yan C, Zang Y. DPARSF: A MATLAB Toolbox for "Pipeline" Data Analysis of Resting-State fMRI. Frontiers in System Neuroscience. 2010; 4: 13.
[45] Yan C, Wang X, Zuo X, Zang Y. DPABI: Data Processing & Analysis for (Resting-State) Brain Imaging. Neuroinformatics. 2016; 14: 339–351.
[46] Marcdante K. Medical College of Wisconsin. Academic Medicine. 2000; 75: S407–S410.
[47] Hayasaka A, Shibahara T, Ito K, Aoki T, Nakajima H, Kobayashi K. A 3D Face Recognition System Using Passive Stereo Vision and its Performance Evaluation. 2006 International Symposium on Intelligent Signal Processing and Communications. IEEE, 2006: 379–382.
[48] Zhang J, Guo Z, Liu X, Jia X, Li J, Li Y, *et al*. Abnormal functional connectivity of the posterior cingulate cortex is associated with depressive symptoms in patients with Alzheimer's disease. Neuropsychiatric Disease and Treatment. 2019; 13: 2589-2598.
[49] Chen HJ, Wang YF, Qi R, Schoepf UJ, Varga-Szemes A, Ball BD, *et al*. Altered Amygdala Resting-State Functional Connectivity in Maintenance Hemodialysis End-Stage Renal Disease Patients with Depressive Mood. Molecular Neurobiology. 2017; 54: 2223-2233.
[50] Beck JR, Shultz EK. The use of relative operating characteristic (ROC) curves in test performance evaluation. Archives of Pathology & Laboratory Medicine. 1986; 110:13–20.
[51] Reynolds S, Carrey N, Jaworska N, Langevin LM, Yang X, Macmaster FP. Cortical thickness in youth with major depressive disorder. BMC Psychiatry. 2014; 14: 83.
[52] Dutta A, McKie S, Deakin JFW. Resting state networks in major depressive disorder. Psychiatry Research. 2015; 224: 139-151.
[53] Fitzgerald DA, Arnold JF, Becker ES, Speckens AEM, Rinck M, Rijpkema M, *et al*. How mood challenges emotional memory formation: an fMRI investigation. NeuroImage. 2011; 56: 1783–1790.
[54] Kim S, Kim YW, Shim M, Jin MJ, Im CH, Lee SH. Altered Cortical Functional Networks in Patients with Schizophrenia and Bipolar Disorder: A Resting-State Electroencephalographic Study. Frontiers in Psychiatry. 2020; 11: 661.
[55] Rabins PV, Pearlson GD, Aylward E, Kumar AJ, Dowell K. Cortical magnetic resonance imaging changes in elderly inpatients with major depression. The American Journal of Psychiatry. 1991; 148: 617–620.
[56] Connolly CG, Ho TC, Blom EH, LeWinn KZ, Sacchet MD, Tymofiyeva O, *et al*. Resting-state functional connectivity of the amygdala and longitudinal changes in depression severity in adolescent depression. Journal of Affective Disorders. 2017; 207: 86–94.
[57] Straub LE, Cisternas MG. Psychological well-being among us adults with arthritis and the unmet need for mental health care. Open Access Rheumatology. 2019; 9: 101–110.
[58] Normann C, Schmitz D, Fürmaier A, Döing C, Bach M. Long-term plasticity of visually evoked potentials in humans is altered in major depression. Biological Psychiatry. 2007; 62: 373–380.
[59] Bueno VF, Brunoni AR, Boggio PS, Bensenor IM, Fregni F. Mood and cognitive effects of transcranial direct current stimulation in post-stroke depression. Neurocase. 2011; 17: 318–322.

Keywords: Psychological distress; Resting-state; Functional neuroimaging; AYACPs; Cancer

Send correspondence to:

Lijun Li, Xiangya Nursing School, Central South University, 410000 Changsha, Hunan, China, E-mail: 197811030@csu.edu.cn

Yunjie Liao, Department of Radiology, The Third Xiangya Hospital, Central South University, 410000 Changsha, Hunan, China, E-mail: liaoyj223@csu.edu.cn

†These authors contributed equally.